Article

FRET Studies of Quinolone-Based Bitopic Ligands and their Structural Analogues at the Muscarinic M1 Receptor

Regina Messerer, Michael Kauk, Daniela Volpato, Maria Consuelo Alonso Cañizal, Jessica Kloeckner, Ulrike Zabel, Susanne Nuber, Carsten Hoffmann, and Ulrike Holzgrabe

ACS Chem. Biol., **Just Accepted Manuscript** • DOI: 10.1021/acschembio.6b00828 • Publication Date (Web): 24 Jan 2017

Just Accepted

ACS Publications

ACS Chemical Biology is published by the American Chemical Society. 1155 Sixteenth Street N.W., Washington, DC 20036

FRET Studies of Quinolone-Based Bitopic Ligands and their Structural Analogues at the Muscarinic M_1 Receptor

Regina Messerer[a, ǂ], Michael Kauk[b, c, ǂ], Daniela Volpato[a], Maria Consuelo Alonso Canizal[b,c], Jessika Klöckner[a], Ulrike Zabel[b,c], Susanne Nuber[b,c], Carsten Hoffmann[b, c, *] and Ulrike Holzgrabe[a, *]

[a] *Department of Pharmaceutical and Medical Chemistry, Institute of Pharmacy, University of Würzburg, Am Hubland, 97074 Würzburg, Germany*

[b] *Department of Pharmacology and Toxicology, University of Würzburg, Versbacher Str. 9, 97078 Würzburg, Germany*

[c] *Rudolf Virchow Center for Experimental Biomedicine, University of Würzburg, Josef Schneider Straße 2, 97080 Würzburg, Germany*

Author Information

[ǂ] R.M. and M.K. contributed equally.

* Corresponding author: e-mail address:

ulrike.holzgrabe@uni-wuerzburg.de (Prof. Dr. Ulrike Holzgrabe); tel.: +49 931 31-85460; fax: +49 931 31-85494.

c.hoffmann@toxi.uni-wuerzburg.de (Prof. Dr. Carsten Hoffmann); tel.: +49 931 31-48304; fax: +49 931 31-48539.

Keywords:

Quinolones, Bitopic ligands, Partial Agonism, Allosteric Modulation, M_1 muscarinic receptor, FRET.

Abbreviations:

ACh, acetylcholine; BQCA, benzyl quinolone carboxylic acid; CFP, cyan fluorescent protein; DAG, diacylglycerol; FlAsH, fluoresceine arsenical hairpin binder; FRET, fluorescence resonance energy transfer; GPCR, G protein-coupled receptor; IL, intracellular loop; M_1, muscarinic acetylcholine subtype 1; mAChR, muscarinic acetylcholine receptor; PAM, positive allosteric modulator; YFP, yellow fluorescent protein.

Abstract

Aiming to design partial agonists as well as allosteric modulators for the M_1 muscarinic acetylcholine (M_1AChR) receptor, two different series of bipharmacophoric ligands and their structural analogues were designed and synthesized. The hybrids were composed of the benzyl quinolone carboxylic acid (BQCA) -derived subtype selective allosteric modulator **3** and the orthosteric building block 4-((4,5-dihydroisoxazol-3-yl)oxy)-N,N-dimethylbut-2-yn-1-amine (base of iperoxo) **1** or the endogenous ligand 2-(dimethylamino)ethyl acetate (base of acetylcholine) **2**, respectively. The two pharmacophores were linked via alkylene chains of different lengths (C4, C6, C8, and C10). Furthermore, the corresponding structural analogues of **1**, **2** and of modified BQCA **3** with varying alkyl chain length between C2 and C10 were investigated. Fluorescence resonance energy transfer (FRET) measurements in a living single cell system were investigated in order to understand how these compounds interact with a G protein-coupled receptor (GPCR) on a molecular level and how the single moieties contribute to ligand receptor interaction. The characterization of the modified orthosteric ligands indicated that a linker attached to an orthoster rapidly attenuates the receptor response. Linker length elongation increases the receptor response of bitopic ligands, until reaching a maximum, followed by a gradual decrease. The optimal linker length was found to be six methylene groups at the M_1AChR. A new conformational change is described that is not of inverse agonistic origin for long linker bitopic ligands and was further investigated by exceptional fragment based screening approaches.

1) Introduction

Muscarinic acetylcholine receptors (mAChRs) belong to class A of G protein-coupled receptors (GPCRs) and are divided into five M receptor subtypes (M_1-M_5). These subtypes regulate the activity of many important functions of the peripheral and central nervous system. They differ in their appearance and physiological function; e.g. the M_1 muscarinic acetylcholine receptor is mostly expressed in the central nervous system (cortex, hippocampus and striatum) and is therefore an interesting therapeutic target for the treatment of Alzheimer`s disease and schizophrenia.[1, 2]

The orthosteric binding pocket appears to be homologues among the five receptor subtypes.[3] This issue is challenging for developing subtype selective therapeutics. To our knowledge Spalding et al.[4] described for the first time an alternative - allosteric binding region at M_1 receptors. This region does not show a high sequence identity and is thus, a promising target for developing subtype selective allosteric modulators. Allosteric modulators can influence the affinity of ligands bound to the topographically distinct orthosteric site, either in a positive, neutral or negative manner.[5] The benzyl quinolone carboxylic acid (BQCA) and their analogues were among others reported by Kuduk et al. to be positive allosteric modulators (PAMs) with respect to orthosteric agonist binding, including the endogenous neurotransmitter acetylcholine, and function in M_1 receptors.[6, 7, 8, 9] To combine the advantages of the two binding sites, the concept of bitopic ligands was developed.[10] These ligands engage the allosteric and orthosteric site simultaneously. Recently, bipharmacophoric ligands consisting of the base of the superagonist iperoxo **1**[11, 12] and a benzyl quinolone carboxylic acid moiety **3** were designed, and found to act as partial *h*M_1 receptor agonists.[13]

For the last two decades a series of different receptor sensors, based on fluorescence resonance energy transfer (FRET), were generated for different GPCRs.[14, 15, 16] Usually, such sensors are tagged C-terminally with cyan fluorescent protein (CFP) and in the third intracellular loop (IL) region with a yellow fluorescent protein (YFP) or a tetracysteine motif capable of binding a small soluble fluorophore called fluoresceine arsenical hairpin binder (FlAsH). These receptor sensors proved to be valuable tools for pharmacological characterizations in intact cells, especially for monitoring receptor activation in real time and to investigate receptor ligand interaction on a molecular level.[17, 18] According to Chen

et al., structure-activity relationships (SARs) showed that the BQCA analogue containing a benzyl moiety at the nitrogen atom as well as a 6-fluoro substituted aromatic ring resulted in a partial *h*M_1 receptor agonist.[13] Due to these findings, the same structural BQCA modification was used for the herein newly designed compounds. Thus, analogues of the superagonist **1**, orthosteric agonist **2**, and of the BQCA-derived subtype selective allosteric modulator **3** were designed, synthesized and characterized, resulting in modified analogues with varying alkyl chain length between C2 and C10 (**1-Cn**, **2-Cn**, and **4-Cn**, where n gives the length of the linker, i.e. the number of C-atoms, Scheme 1 and Scheme 2). The attachment point was chosen on the tetramethyl moiety as this group points out of the orthosteric binding pocket as seen for iperoxo.[19] Furthermore, the fluoro-substituted allosteric BQCA moieties were linked to the base of orthosteric agonists iperoxo and to the base of acetylcholine, aiming to design bipharmacophoric M_1 receptor agonists (**5-C** and **6-C**, Scheme 2). The linker elongation on the BQCA modified pharmacophore was attached on the carboxylic acid residue due to molecular modeling studies suggesting that the carboxylic acid position points out toward the extracellular site of the receptor.[20] Furthermore, the carboxylic moiety is a suitable attachment point for improving allosteric modulation. For the pharmacological characterization of these ligands a novel M_1 FRET sensor was used. This study provides an insight into M_1 receptor activation, receptor conformational changes monitored by the movement of fluorescent labeled domains, and signaling behavior.

2) RESULTS AND DISCUSSION

2.1) Chemistry. The reaction sequences of the iperoxo analogues **1-C2** to **1-C10** and of the acetylcholine analogues **2-C4**, **2-C6**, **2-C8**, and **2-C10** are illustrated in Scheme 1. 4-((4,5-dihydroisoxazol-3-yl)oxy)-*N*,*N*-dimethylbut-2-yn-1-amine[11] (base of iperoxo) **1** and 2-(dimethylamino)ethyl acetate (base of acetylcholine) **2**, respectively, were reacted with the corresponding bromoalkane in acetonitrile, affording the final monoquaternary ammonium salts **1-C2** to **1-C10** and **2-C4**, **2-C6**, **2-C8**, and **2-C10** in 48-91% yield. The synthesis of the acetylcholine analogues **2-C4**, **2-C6**, and **2-C8** were described previously using a different synthetic pathway.[21]

Insertion of Scheme 1 about here

As already reported, the fluoro-4-oxo-quinolone skeleton of **8** was synthesized using the Gould-Jacobs procedure, starting off with the condensation of 4-fluoroaniline with diethyl 2-(ethoxymethylene)-malonate and subsequent cyclization in boiling diphenyl ether.[22, 23, 24] Ester hydrolysis led to compound **3**.[25] Conversion of the ester function (**9**) with the aminoalcohols of the corresponding spacer length (C4, C6, C8, C10), substitution of the alcohol function with a bromine atom using HBr/H_2SO_4 and subsequent reaction with trimethylamine in acetonitrile at 40 °C led to the monoquaternary ammonium salts **4-C4**, **4-C6**, **4-C8**, and **4-C10** in 53-96% yield. For the preparation of the final BQCA/iperoxo hybrids **5-C4**, **5-C6**[13], **5-C8**, and **5-C10** as well as the BQCA/ACh hybrids **6-C4**, **6-C6**, **6-C8**, and **6-C10**, the intermediate bromides were connected to the base of iperoxo and to the base of acetylcholine, respectively, in the presence of KI/K_2CO_3 in acetonitrile (Scheme 2).

Insertion of Scheme 2 about here

2.2) Pharmacology/Fret measurements

2.2.1) Receptor sensor and ligand characterization. In comparison to the previously reported M_1-, M_3-, M_5-[26] and M_2-ACh receptor FRET-sensors [27], we created a novel full length FRET sensor of the human M_1-ACh receptor which was not truncated in the 3rd intracellular loop (IL3). This novel sensor consists of the native amino acid sequence fused at the receptor C-terminus to CFP by adding the amino acids Ser/Arg encoding for an XbaI site. Additionally, a FlAsH binding motif CCPGCC was inserted between Gly227 and Ser228 (Fig. 1a) at the N-terminal part of IL3 shortly underneath transmembrane domain 5 outside of the G protein-coupling region.[28] The receptor construct M1-I3N-CFP expressed well at the cell surface as analyzed by confocal scanning laser microscopy (Supplementary Figure 1). Since the previously published truncated sensors were not different from wild-type receptors in radioligand binding,[17] we characterized only functional response of the novel sensor. To evaluate the effect of the six amino acid insertion into the M1-CFP receptor we used a dual fluorescence probe, which responds with an increase in red

fluorescence intensity upon increase in Ca^{2+} and a decrease in green fluorescence upon binding to diacylglycerol (DAG). Therefore, the probe can specifically report on the activation of Gq-signalling.[29] The dual fluorescent probe was transfected in HEK293 cells either alone or co-expressed with the M1-CFP or the novel M1-I3N-CFP sensor and analyzed by confocal microscopy (see supplementary information for details). The dual probe did not respond to carbachol if no receptor was co-transfected. As shown in Supplementary Figure 2 the carbachol stimulated response was indistinguishable for the M1-CFP receptor or the M1-I3N-CFP sensor. In combination with previous binding experiments on a truncated sensor version[17] it was concluded that this sensor is not disturbed in its signaling properties by insertion of the CCPGCC sequence. For further FRET experiments the M1-I3N-CFP was stably expressed in HEK293 cells and single cells were used for further analysis. To study dynamic conformational changes in real time the M1-I3N-CFP sensor was exposed to the endogenous agonist ACh and the synthetic full agonist iperoxo. To eliminate potential artefacts from changes in flow rates, the cells were constantly superfused with buffer. Under these conditions the receptor sensor shows a constant baseline. Upon ligand addition a sharp antiparallel movement of the CFP and FlAsH signal was observed (Supplementary Figure 3), resulting in a concentration dependent change in the FRET signal of 8-12% for iperoxo (Fig. 1b). When the superfusion solution was switched back from agonist to buffer, the signal returned to the baseline. A slight reduction of the FRET signal over time was detectable and could be due to photobleaching. To prevent artificial underestimation of ligand efficacy reference and ligand were measured in an alternating exposure regime. Thus, we were able to generate concentration dependent response (Fig. 1c) curves for the endogenous agonist ACh (EC_{50} = 2.91 µM) and the synthetic full agonist iperoxo (EC_{50} = 0.57 µM). The observed EC_{50} value for ACh is in very good agreements with previously obtained value using the truncated receptor sensor.[17] Due to a five-fold higher potency of iperoxo compared to ACh, the base of iperoxo **1** was chosen as the orthosteric building block for the studied bitopic ligands to ensure high receptor activation via the orthosteric binding site.

As allosteric building block a structural analogue of benzyl quinolone carboxylic acid (BQCA) origin was chosen. In 2009, BQCA was reported to be a M_1 selective positive allosteric modulator (PAM)[9] whose binding region was studied in detail.[20] However, an essential property of allosteric modulators is probe dependency. Thus, an experimental

approach to show this cooperative effect of BQCA analogue (**3**) combined with iperoxo (Fig. 1d) was designed. To study positive modulation, a concentration of iperoxo which results in approximately 20% of the maximal observed signal (EC_{20}) was chosen. This way a clear signal was observed and still a large detection range to observe positive allosteric modulation was available. As seen in Figure 1d by applying the allosteric modulator **3** alone, a small conformational change was found. This small response was not clearly detectable for all cells measured. This might be explained by the very small signal that could not always be distinguished from noise. When applying saturating concentrations of iperoxo, a significant signal was monitored. Next iperoxo at 0.1 µM concentration was applied which results in 25% signal compared to saturating ligand concentrations. Now the superfusion was changed to a mix of iperoxo and **3** and again back to iperoxo alone. A clear enhanced receptor response was observed by applying **3** and iperoxo at the same time, compared with the appropriate iperoxo response. This enhanced response is higher than a theoretical additive effect of the conformational changes induced by **3** and iperoxo alone and can be described as positive allosteric modulation.

2.2.2) Linker elongation attenuates orthosteric properties. Besides their orthosteric and allosteric moieties, bitopic ligands consist of a linker region that is often not investigated in a systematic way and hence, the linker is often inappropriately treated. To date the molecular effects of additional carbon atoms at an orthosteric ligand for muscarinic receptors are still unknown. Therefore, nine different structural analogues of **1** with a linker attached to the amine group were synthesized (Scheme 1, **1-C2** to **1-C10**). These compounds were investigated via FRET for their ability to induce a conformational change at the M_1 receptor. The results are summarized in Figure 2. Figure 2a shows a single FRET experiment comparing the effect of iperoxo and different concentrations of **1-C2** and **1-C3**. Even saturating concentrations of **1-C2** exhibit a much reduced FRET signal compared to the reference compound iperoxo. From these data it can be concluded, that additional methylene units significantly reduce the efficacy to 65% compared to iperoxo. Nonetheless it was possible to generate a concentration response curve for **1-C2**. Besides the reduced efficacy a 3-fold lower affinity (EC_{50} (**1-C2**) = 1.65 µM) to the receptor sensor became evident (Fig. 2b). For **1-C3** a more than 80% reduced conformational change was found. These signals were too small to establish a reliable concentration response curve. The iperoxo analogues (**1-C4** to **1-C10**) did not induce any conformational change at the

receptor sensor (Fig. 2c). In order to test, whether the linker extended ligands were able to bind the receptor sensor at the orthosteric binding site, competition experiment were performed shown in Figure 2d. To test for binding of **1-C6** first 10 µM of iperoxo as a concentration which induces 80% of the maximal signal response (EC_{80}) was applied. In the first case a single ligand to the receptor sensor was superfused (Fig 2d). Next, a 10 µM solution of iperoxo with 100 µM of the linker analogue **1-C6** was added. As can be seen in Figure 2d, the receptor response induced by the ligand mix was significantly reduced compared to the signal induced by iperoxo alone, most likely indicating, that the two ligands compete for the orthosteric binding site and that the **1-C6** analogue shows affinity to the orthosteric binding site but does not exhibit efficacy as shown by the lack of conformational changes in Figure 2c. In Figure 2e the results for a corresponding set of ligands of ACh origin (Scheme 1) is displayed. The given FRET trace proves, that a distinct linker elongation at an orthosteric ligand attenuates orthosteric efficacy. This phenomenon could be due to a steric hindrance within the binding pocket or due to preventing an essential receptor movement like closing the aromatic lid, which was proposed before to be essential for receptor activation.[19]

2.2.3) Evaluation of Bitopic ligands. Bitopic ligands are thought to interact with both orthosteric and the allosteric binding site at the same time.[10] They are also thought to interact with the receptor in a dynamic binding mode, which consist at least of two different states.[30, 31] Abdul-Ridha et al.[20] investigated both binding sites in great detail by mutational analysis. Using this approach, it was possible to restrict the relative position of both moieties to a certain area of the receptor.[20] In combination with the crystal structure of iperoxo bound to the M_2-receptor subtype[19] and the recently published crystal structure of the M_1-receptor subtype[3], we focused on bitopic ligands with different linker length consisting of either four, six, eight or ten carbon atoms. Thus, these ligands cover a relative distance of 6 Å to 15 Å between both pharmacophore moieties and hence representing the seven transmembrane helical core. A series of bitopic ligands consisting of the base of iperoxo (**1**) and the BQCA analogue (**3**) were synthesized (Scheme 2). Correspondingly these ligands are called **5-Cn** with **n** reflecting the linker length (**4**, **6**, **8**, **10**) (Scheme 2). As can be seen in Figure 3a, showing a representative FRET trace of **5-C6**, clear concentration dependent increase in conformational change has taken place. This is the largest conformational change at this FRET sensor compared to all

other structural analogues in this series. All other ligands were also able to induce a conformational change at the M_1 receptor sensor. Figure 3b shows the maximal ligand induced changes in comparison to iperoxo. The dashed line indicates the maximal observed signal for the allosteric moiety **3** when tested alone. Since all corresponding iperoxo linker analogues (**1-C4** to **1-C10**) alone did not induce a conformational change (cf. Fig. 2c), the difference in conformational changes of the hybrids above the dashed line should either result from the positive cooperativity between the orthosteric and allosteric moieties, or an alternative binding pose. Moreover, for the M_1 receptor the optimal linker length for the combination of **1** and **3** is in the range of six methylene groups (see Fig. 3b), whereas for the M_2-receptor subtype longer linker lengths are necessary to improve bitopic ligand efficacy.[30] Thus, the optimal linker length as well as the nature of the linker chain are crucial for receptor activation and are different for each receptor subtype, depending on their tertiary structure. A first indication for receptor subtype selectivity among acetylcholine receptors is shown in supplementary figure 4. Compound **5-C6** was tested at a previously published M_3-ACh receptor FRET sensor[26] and did not evoke a conformational change as observed for iperoxo. Furthermore, after reaching an optimal linker length, the efficacy of bitopic ligands decline by further linker elongation (Fig. 3b). Surprisingly, when investigating compound **5-C10** a concentration dependent signal with opposite signal direction compared to iperoxo was found (Fig. 3C). Since changes in FRET signals in general represent a relative distance change this property was used as a readout for conformational changes at GPCRs. The opposite FRET signal induced by **5-C10** was not observed before for any bitopic ligand at M-receptors. Comparable inverse FRET signals were reported for inverse agonistic responses at constitutively active mutants of the α_{2a} adrenergic receptor[32] and the M_3 mutant[33]. At constitutively active M_3 receptors, atropine behaves as an inverse agonist. Hence, to compare the effect found for **5-C10** at the M1-I3N-CFP with eventual constitutive activity, the effect of atropine at this construct was studied. However, neither atropine nor tiotropium did induce any conformational change (see Fig. 3d or Supplementary Figure 5), arguing against constitutive activity as an explanation for the behavior of **5-C10**. Of note, the high receptor affinity of atropine becomes visible by the fact, that it was almost impossible to induce a second signal for iperoxo after the first application of 10 µM atropine. To further study the surprising effect of **5-C10**, a series of bitopic ligands based

on acetylcholine as orthosteric building block **6-C4** to **6-C10** (Scheme 2) was investigated. Figure 3e displays a representative FRET trace of acetylcholine based bitopic ligands and the bar graph in Figure 3f summarizes the measured FRET-signals. Again a linker length dependent receptor response was found. Moreover, again inverse FRET-signals for bitopic ligands of longer chain length were detected. Interestingly, for this compound series a FRET-signal with similar direction as observed for ACh was never detected.

2.2.4) Linker fusion at the allosteric building block. In order to find out, why bitopic ligands with longer linkers produce an inverse FRET signal it was of interest to unravel the moiety of the ligands contributing to the observed signals. Additionally, the question arose whether it would be possible to reconstruct the signal derived by different bitopic ligands by combining the individual components in a fragment-based screening approach in a single cell. Therefore, the ligands **5-C6** and **5-C10** who showed the most extreme signals were studied. As shown in Figure 1d the BQCA analogue (**3**) induces a small conformational change but the corresponding linker extended iperoxo analogue (**1-C6**) did not exhibit a detectable effect at our receptor sensor (Fig. 2c), but **1-C6** binds to the receptor (Fig. 2d). Both effects are shown in Figure 4a, this time measured at the same cell. By applying both compounds (**3** and **1-C6**) at the same time a receptor response was observed that was on the one hand significantly different to the BQCA response but on the other hand similar in the maximal signal intensity as reported before for the bitopic ligand **5-C6** (Fig. 3a), indicating first that it is possible to reconstruct the effect of a bitopic ligand interacting with a receptor by applying the fragments at the same time to the receptor sensor, and second that there is cooperativity between the allosteric modulator BQCA (**3**) and the ligand **1-C6**, which showed high affinity to the orthosteric binding site.

Comparable experiments were performed with the ligand **5-C10** and its respective building blocks (Fig. 4b). Interestingly in this case it was impossible to reconstruct the signal of the bitopic ligand by applying the single fragments, suggesting, that the inverse signal is likely mechanistically different to the agonistic signal. Interestingly at the M_2 mAChR, iperoxo-based bitopic ligands have been shown to bind in at least two different binding poses[31] and one of them was shown to be purely allosteric. This has recently been further investigated by molecular modeling.[34] In an attempt to explain the inverse FRET signal mechanistically, the set of compounds **4-C4** to **4-C10**, consisting of the allosteric

moiety, was studied. Here a linker moiety of different length and a tertiary amine are combined to imitate the positively charged amine of the orthosteric ligand (Scheme 2) in the presence of the allosteric moiety. Figure 4c displays a representative FRET trace recorded for a single cell that was super-fused with the indicated ligands. Increasing linker length lead to the appearance of an inverse signal for compound **4-C8** and **4-C10** even in the absence of the orthosteric moiety similar to the signal observed for compound **5-C10** or **6-C10**. This result supports the notion of an alternative second binding pose for the linker extended bitopic ligands at the M_1 receptor, as recently described for the M_2 receptor.[34] Another hypothesis is the possible binding of the ligands to two allosteric binding sites in a dimeric receptor.[35]

2.3) Concluding remarks. Bitopic ligands are molecular entities, which bind to more than one pharmacological interesting region of membrane proteins and are thought to have an impact on further drug development. This study provides a molecular insight of the interactions between GPCRs and bitopic ligands for a better understanding of ligand receptor interactions on a molecular level. Here, linker dependent responses of bitopic ligands at a M_1 receptor FRET sensor were investigated. The findings indicate an optimal linker length of the bitopic ligands for conformational changes at the M_1 mAChR. This optimal linker length is probably different for each receptor subtype and is likely dependent on the individual receptor architecture. Furthermore, a previously unknown conformational change for GPCRs induced by bitopic ligands of long linker length was observed. Furthermore, an understanding of the origin of different conformational changes of GPCRs is provided. The influences of the reported movements on the downstream signaling of GPCRs are subjects of current studies. Bitopic ligands were discussed critically due to the fact, whether the lipophilic linker can pass the aromatic lid of muscarinic receptors. Here, it could be shown that an increased linker first hampers the orthoster to induce a conformational change although there is a distinct affinity to the orthosteric binding region. This phenomenon might be due to a steric clash with the aromatic lid structure in muscarinic acetylcholine receptors. Moreover, the findings indicate, that this fact is no longer true for the bitopic analogues indicating that here the linker is able to interact with the aromatic lid without being sterically hindered.

3) METHODS

3.1) Chemistry. Melting points were determined with a Stuart melting point apparatus SMP3 (Bibby Scientific) and are uncorrected. ^{1}H (400.132 MHz) and ^{13}C (100.613 MHz) NMR spectra were recorded on a Bruker AV 400 instrument (Bruker Biospin). As internal standard, the signals of the deuterated solvents were used (DMSO-d_6: ^{1}H 2.5 ppm, ^{13}C 39.52 ppm; $CDCl_3$: ^{1}H 7.26 ppm, ^{13}C 77.16 ppm). Abbreviation for data quoted are: s, singlet; d, doublet; t, triplet; q, quartet; m, multiplet; b, broad; dd, doublet of doublets; dt, doublet of triplets; tt, triplet of triplets; tq, triplet of quartets. Coupling constants (*J*) are given in Hz. TLC analyses were performed on commercial pre-coated plates, silica gel 60 F_{254} (Macherey-Nagel); spots were further evidenced by spraying with Dragendorff reagent,[36] for amines. ESI mass spectra of the compounds were obtained on an Agilent LC/MSD Trap G2445D instrument. Data are reported as mass-to-charge ratio (*m/z*) of the corresponding positively charged molecular ions. Microwave assisted reactions were carried out on a MLS-rotaPREP instrument (Milestone). Chemicals were of analytical grade and purchased from Aldrich and Merck.

The purities of the compounds (**2-C4**, **2-C6**, **2-C8**, and **2-C10**) were determined using qNMR and were found to be ≥95% (method see supporting information). Purity of compounds **1-C2**, **1-C6**, **1-C7**, **1-C8**, **1-C9**, **1-C10**, **5-C4**, and **6-C6** were determined using capillary electrophoresis and were found to be ≥95% (method see supporting information). Compounds **1-C4** and **6-C4** (confirming purity ≥95%) and compounds **5-C8** and **5-C10** (confirming purity ≥90%) were measured on a HPLC system (Agilent 1100 series system with UV detector) using a C18 reversed-phase (Knauer) (150 x 4.6 mm) column. The mobile phase (MeOH/phosphate buffer = 70/30) was used at a flow rate of 1.5 mL/min, detecting at 254 nm. The HPLC analyses of compounds **4-C4** (confirming purity ≥90%) **4-C6**, **4-C8**, **4-C10**, **6-C8**, and **6-C10** (confirming purity >95%) were performed on a LCMS 2020 Shimadzu. The LCMS-system from Shimadzu Products, contained a DGU-20A3R degassing unit, a LC20AB liquid chromatograph and a SPD-20A UV/Vis detector. Mass spectra were obtained by a LCMS 2020. As stationary phase a Synergi 4U fusion-RP (150 * 4.6 mm) column and as mobile phase a gradient of MeOH/water was used. Parameters for method: Solvent A: water with 0.1% formic acid, solvent B: MeOH with

0.1% formic acid. Solvent B from 0% to 90% in 13 min, then 90% for 5 min, from 90% to 5% in 1 min, then 5% for 4 min. The method was performed with a flow rate of 1.0 mL/min. UV detection was measured at 254 nm.

The compounds **1-C3**, **1-C5**,[12] and **3**[25] as well as **9**, **10-C6**, **11-C6**, and **5-C6**[13] were prepared according to previously reported procedures. The synthesis of the 4-oxo-quinoline skeleton **8**[37, 38] was performed in analogy to the Gould-Jacobs procedure, using diethyl 2-(ethoxymethylene)-malonate for the condensation with 4-fluoroaniline followed by microwave assisted cyclization in diphenyl ether.[22, 23, 24]

3.1.1) General Procedure for the Synthesis of the Iperoxo Analogues 1-C2, 1-C4, 1-C6, 1-C7, 1-C8, 1-C9, and 1-C10. To a solution of 4-((4,5-dihydroisoxazol-3-yl)oxy)-*N*,*N*-dimethylbut-2-yn-1-amine[11] 0.45 g (2.47 mmol) in 10 mL of acetonitrile or chloroform, 5 - 10 equivalents of the corresponding 1-bromoalkane **7-C2** to **7-C10** and a catalytic amount of KI/K_2CO_3 (1:1) were added. The mixture was stirred in a sealed container at a temperature between 55 and 70 °C. The precipitate obtained was filtered and Et_2O was added to complete the precipitation. The solid was washed several times with Et_2O, and dried over P_2O_5 in vacuo.

3.1.2) General Procedure for the Synthesis of the Acetylcholine Analogues 2-C4, 2-C6, 2-C8, and 2-C10. To a solution of 2-(dimethylamino)ethyl acetate 0.50 g (3.81 mmol) in acetonitrile (10 mL), 2 equiv. of the corresponding 1-bromoalkane **7-C4**, **7-C6**, **7-C8**, and **7-C10** and a catalytic amount of KI/K_2CO_3 (1:1) were added. The reaction mixture was heated in the microwave (500 W, 70 °C) for 4 h. After cooling to room temperature the surplus of KI/K_2CO_3 was filtered and the filtrate was evaporated to the half of the volume. After addition of Et_2O, a viscous oil was formed. The solvent was decanted and the product obtained was dried in vacuo.

3.1.3) General Procedure for the Synthesis of the Quinolone Analogues 4-C4, 4-C6, 4-C8, and 4-C10. To a solution of bromoalkyl 4-oxo-quinoline-3-carboxamides **11-C4**, **11-C6**, **11-C8**, and **11-C10** (0.11 mmol) in acetonitrile (5 mL), trimethylamine (45% in H_2O, 0.22

mmol) was added. The reaction was heated at 40 °C. After completion of the reaction (5 h) controlled by TLC (CH_2Cl_2/MeOH = 85:15, R_f = 0.10 – 0.45), the mixture was cooled to room temperature. The solvent was distilled off. The so obtained solid was crystallized from acetonitrile, filtered and dried in vacuo.

3.1.4) General Procedure for the Synthesis of the Quinolone-Iperoxo Hybrids 5-C4, 5-C8, and 5-C10. To a solution of 1 equiv. of the bromoalkyl 4-oxo-quinoline-3-carboxamides **11-C4**, **11-C8**, and **11-C10** in 20 mL acetonitrile, 2 equiv. 4-((4,5-dihydroisoxazol-3-yl)oxy)-*N*,*N*-dimethylbut-2-yn-1-amine[11] and a catalytic amount of KI/K_2CO_3 (1:1) were added. The reaction mixture was heated in the microwave (500 W, 80 °C) for 4 h. The reaction was monitored by TLC (MeOH/NH_4NO_2 (0.2 M) = 3:2, R_f = 0.54 – 0.68). After cooling to room temperature the surplus of KI/K_2CO_3 was filtered. Et_2O was added to the filtrate to obtain a precipitation. The solid was filtered, washed with Et_2O and dried in vacuo.

3.1.5) General Procedure for the Synthesis of the Quinolone-Acetylcholine Hybrids 6-C4, 6-C6, 6-C8, and 6-C10. To a solution of 1 equiv. of the bromoalkyl 4-oxo-quinoline-3-carboxamides **11-C4**, **11-C8**, and **11-C10** in 15 mL acetonitrile, 2 equiv. 2-(dimethylamino)ethyl acetate and a catalytic amount of KI/K_2CO_3 (1:1) were added. The reaction mixture was heated in the microwave (500 W, 80 °C) for 4.0 – 6.5 h. After cooling to room temperature the surplus of KI/K_2CO_3 was filtered and Et_2O was added to the filtrate. The solid obtained was filtered, washed with Et_2O and dried in vacuo.

3.2) Pharmacology

3.2.1) Construction of the *h*M_1 receptor FRET sensor. Muscarinic ACh receptor construct was C-terminally fused to the enhanced variants of cyan fluorescent protein (eCFP) (BD Bioscience Clontech) by standard PCR extension overlap technique.[39] The amino acid sequence SR, coding for an Xba I restriction site, was inserted as a linker sequence between receptor and fluorescent protein. In the third intracellular loop (IL3) an amino acid motif was introduced, thus the novel sequence reads QG227CCPGCCSGS228E. It specifically binds the fluorescein arsenical hairpin binder (FlAsH) and codes for a

restriction site. The construct was cloned into pcDNA3 (Invitrogen) and verified by sequencing, done by Eurofins Genomics.

3.2.2) Stable cell line generation. Cells were seeded into a culture dish with a confluency of 30% three hours before transfecting the cells with the Effectene® reagent ordered from Quiagene. Reagent concentration and incubation times were applied in accordance with the manufacturer's instructions. 24 hours after transfecting the normal culture medium was replaced by culture medium supplemented with 400 µg mL^{1} G-418. After that the medium was refreshed every day until all untransfected cells died. Now the cells were counted, diluted and applied to 48-well plates resulting in a one cell to well distribution. This homogenous cell population were characterized with fluorescence microscopy and were investigated concerning their cDNA content.

3.2.3) Cell culture. HEK293 cells stably expressing the *h*M_1 receptor FRET sensor were maintained in DMEM with 4.5 g l^{1}, 10% (v/v) FCS, 100 U mL^{1} penicillin, 100 µg mL^{1} streptomycin sulfate and 2 mM L-glutamine and 200 µg mL^{1} G-418. The cells were kept at 37 °C in a humidified 7% CO_2 atmosphere and were routinely passaged every two to three days. Untransfected HEK cells maintained in cell culture medium without G-418.

3.2.4) FlAsH labeling. A labeling protocol was applied as described previously.[15, 40, 41] In brief, cells were grown to near confluency on Poly-D-lysine coated glass coverslips. Initially cells were washed with labeling buffer (150 mM NaCl, 10 mM HEPES, 2.5 mM KCl, 4 mM $CaCl_2$, 2mM $MgCl_2$ supplemented with 10 mM glucose (pH 7.3)). After that cells were incubated with labeling buffer containing 500 nM FlAsH and 12.5 µM 1,2-ethanedithiol (EDT) for 1 h at 37 °C followed by flushing with labeling buffer. To reduce non-specific FlAsH binding, the cells were incubated for 10 min with labeling buffer containing 250 µM EDT. After flushing with labeling buffer the cells were held in cell culture medium.

3.2.5) Ligand application. The reference ligands were prepared from 1 mM stock solutions that were stored at -20 °C, taking into consideration, that at least acetylcholine remains instable in solution.[42] Used stock solutions have not been older than a couple of weeks. Bitopic ligands or analogues were stored at 4 °C and were weighed out directly before the experiment. Than the ligands were solubilized in measuring buffer (140 mM NaCl, 10 mM HEPES, 5.4 mM KCl, 2 mM $CaCl_2$, 1 mM $MgCl_2$ (pH 7.3)) to a final concentration of 100 µM.

3.2.6) Single cell FRET experiments. FRET measurements were performed using a Zeiss Axiovert 200 inverted microscope endued with a PLAN-Neoflar oil immersion 100-objective, a dual emission photometric system and a Polychrome IV light source (Till Photonica) as described previously.[15, 14] Experiments were conducted at 25 °C using live HEK293 cells stably expressing the *h*M_1 receptor FRET-sensor or the previously published *h*M_3 receptor FRET-sensor[26] that were maintained in assay buffer. Single cells were excited at 436 nm (dichroic 460 nm) with a frequency of 10 Hz. Emitted light was recorded using 535/30 nm and 480/40 nm emission filters and a DCLP 505 nm beam splitter for FlAsH and CFP, respectively. FRET was observed as the ratio of FlAsH/CFP, which was corrected offline for bleed through, direct FlAsH excitation and photo bleaching using the 2015 version of the Origin software as described recently. To investigate changes in FRET on ligand addition, cells were continuously super fused with FRET buffer complemented with various ligands in saturating concentrations as indicated. Superfusion was done using the ALA-VM8 (ALA Scientific Instruments).

3.2.7) Data processing. Data are shown as means ± SD for n independent observations. Fluorescence intensities were acquired using Clampex (Axon Instruments). Statistical analysis and curve fitting were performed using Origin (OriginLab).

Supporting Information

Supporting Information Available: This material is available free of charge *via* the internet. More detailed syntheses, elemental analyses data and spectral data of intermediate and target compounds as well as calcium measurement procedure description and supporting figures.

Acknowledgements

M. Kauk and D. Volpato were supported by the international doctoral college "Receptor Dynamics: Emerging Paradigms for Novel Drugs" funded within the framework of the Elite Network of Bavaria. M.C. Alonso Canizal was supported by the Marie Curie Initial Training Networks (ITN) "WntsApp" grant agreement number 608180. We thank Montana Molecular and Dr. Anne Marie Quinn for technical support and help to use the dual sensor.

Scheme 1: Synthesis of orthosteric M_1 agonist agents based on Iperoxo – and Acetylcholine Analogues.

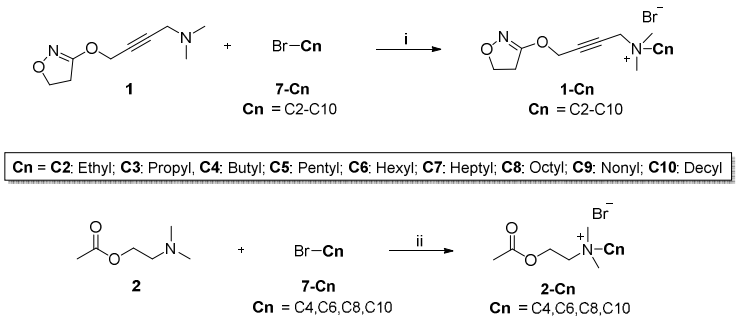

Reagents and conditions: (i) KI/K_2CO_3, $CH_3CN/CHCl_3$, 70 °C (48-89%); (ii) KI/K_2CO_3, CH_3CN, 70 °C (microwave) (65-91%).

Scheme 2: Synthesis of Quinolone Analogues, BQCA/Iperoxo Hybrids and BQCA/ACh Hybrids.

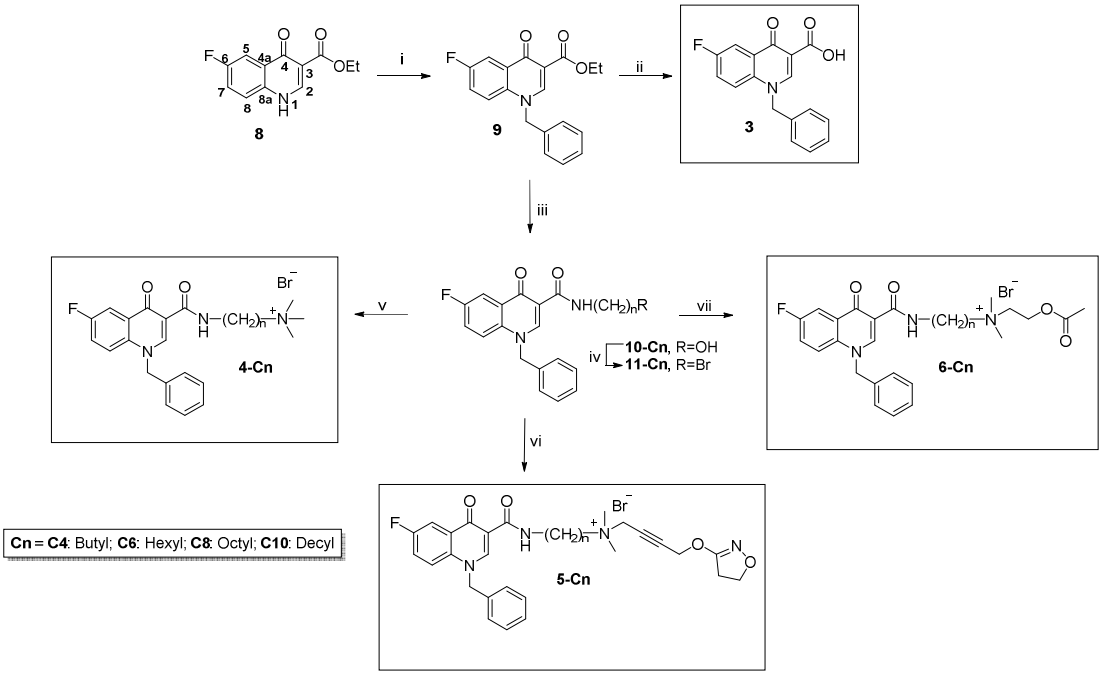

Reagents and conditions: (i) benzyl chloride, K_2CO_3, DMF, 80 °C (72%); (ii) 6 N HCl, MeOH, reflux (77%); (iii) $H_2N(CH_2)_nOH$, 150 °C (28-33%); (iv) HBr (48%), H_2SO_4, reflux (73-93%); (v) trimethylamine, CH_3CN, 40 °C (53-96%); (vi) **1**, KI/K_2CO_3, CH_3CN, 80 °C (microwave) (37-66%); (vii) **2**, KI/K_2CO_3, CH_3CN, 80 °C (microwave) (19-73%).

References

[1] Wess, J. (2004) Muscarinic acetylcholine receptor knockout mice: novel phenotypes and clinical implications, *Annu. Rev. Pharmacol. Toxicol. 44*, 423-450.

[2] Kruse, A. C., Kobilka, B. K., Gautam, D., Sexton, P. M., Christopoulos, A., and Wess, J. (2014) Muscarinic acetylcholine receptors: novel opportunities for drug development, *Nat. Rev. Drug. Discov. 13*, 549-560.

[3] Thal, D. M., Sun, B., Feng, D., Nawaratne, V., Leach, K., Felder, C. C., Bures, M. G., Evans, D. A., Weis, W. I., Bachhawat, P., Kobilka, T. S., Sexton, P. M., Kobilka, B. K., and Christopoulos, A. (2016) Crystal structures of the M1 and M4 muscarinic acetylcholine receptors, *Nature 531*, 335-340.

[4] Spalding, T. A. (2002) Discovery of an Ectopic Activation Site on the M1 Muscarinic Receptor, *Mol. Pharmacol. 61*, 1297-1302.

[5] De Amici, M., Dallanoce, C., Holzgrabe, U., Tränkle, C., and Mohr, K. (2010) Allosteric ligands for G protein-coupled receptors: a novel strategy with attractive therapeutic opportunities, *Med. Res. Rev. 30*, 463-549.

[6] Mistry, S. N., Valant, C., Sexton, P. M., Capuano, B., Christopoulos, A., and Scammells, P. J. (2013) Synthesis and pharmacological profiling of analogues of benzyl quinolone carboxylic acid (BQCA) as allosteric modulators of the M1 muscarinic receptor, *J. Med. Chem. 56*, 5151-5172.

[7] Kuduk, S. D., Chang, R. K., Di Marco, C. N., Ray, W. J., Ma, L., Wittmann, M., Seager, M. A., Koeplinger, K. A., Thompson, C. D., Hartman, G. D., and Bilodeau, M. T. (2010) Quinolizidinone carboxylic acids as CNS penetrant, selective m1 allosteric muscarinic receptor modulators, *ACS Med. Chem. Lett. 1*, 263-267.

[8] Davie, B. J., Valant, C., White, J. M., Sexton, P. M., Capuano, B., Christopoulos, A., and Scammells, P. J. (2014) Synthesis and pharmacological evaluation of analogues of benzyl quinolone carboxylic acid (BQCA) designed to bind irreversibly to an allosteric site of the M (1) muscarinic acetylcholine receptor, *J. Med. Chem. 57*, 5405-5418.

[9] Ma, L., Seager, M. A., Wittmann, M., Jacobson, M., Bickel, D., Burno, M., Jones, K., Graufelds, V. K., Xu, G., Pearson, M., McCampbell, A., Gaspar, R., Shughrue, P., Danziger, A., Regan, C., Flick, R., Pascarella, D., Garson, S., Doran, S., Kreatsoulas, C., Veng, L., Lindsley, C. W., Shipe, W., Kuduk, S., Sur, C., Kinney, G., Seabrook, G. R., and Ray, W. J. (2009) Selective activation of the M1 muscarinic acetylcholine receptor achieved by allosteric potentiation, *Proc. Natl. Acad. Sci. U. S. A. 106*, 15950-15955.

[10] Mohr, K., Schmitz, J., Schrage, R., Tränkle, C., and Holzgrabe, U. (2013) Molecular alliance-from orthosteric and allosteric ligands to dualsteric/bitopic agonists at G protein coupled receptors, *Angew. Chem. Int. Ed. Engl. 52*, 508-516.

[11] Kloeckner, J., Schmitz, J., and Holzgrabe, U. (2010) Convergent, short synthesis of the muscarinic superagonist iperoxo, *Tetrahedron Lett. 51*, 3470-3472.

[12] Schrage, R., Seemann, W. K., Kloeckner, J., Dallanoce, C., Racke, K., Kostenis, E., De Amici, M., Holzgrabe, U., and Mohr, K. (2013) Agonists with supraphysiological efficacy at the muscarinic M2 ACh receptor, *Br. J. Pharmacol. 169*, 357-370.

[13] Chen, X., Kloeckner, J., Holze, J., Zimmermann, C., Seemann, W. K., Schrage, R., Bock, A., Mohr, K., Tränkle, C., Holzgrabe, U., and Decker, M. (2015) Rational design of partial agonists for the muscarinic m1 acetylcholine receptor, *J. Med. Chem. 58*, 560-576.

[14] Vilardaga, J. P., Bünemann, M., Krasel, C., Castro, M., and Lohse, M. J. (2003) Measurement of the millisecond activation switch of G protein-coupled receptors in living cells, *Nat. Biotechnol. 21*, 807-812.

[15] Hoffmann, C., Gaietta, G., Bünemann, M., Adams, S. R., Oberdorff-Maass, S., Behr, B., Vilardaga, J. P., Tsien, R. Y., Ellisman, M. H., and Lohse, M. J. (2005) A FlAsH-based FRET

approach to determine G protein-coupled receptor activation in living cells, *Nat. Methods 2*, 171-176.

[16] Stumpf, A. D., and Hoffmann, C. (2016) Optical probes based on G protein-coupled receptors - added work or added value?, *Br. J. Pharmacol. 173*, 255-266.

[17] Vilardaga, J. P., Bünemann, M., Feinstein, T. N., Lambert, N., Nikolaev, V. O., Engelhardt, S., Lohse, M. J., and Hoffmann, C. (2009) GPCR and G proteins: drug efficacy and activation in live cells, *Mol. Endocrinol. 23*, 590-599.

[18] Lohse, M. J., Nuber, S., and Hoffmann, C. (2012) Fluorescence/bioluminescence resonance energy transfer techniques to study G-protein-coupled receptor activation and signaling, *Pharmacol. Rev. 64*, 299-336.

[19] Kruse, A. C., Ring, A. M., Manglik, A., Hu, J. X., Hu, K., Eitel, K., Hübner, H., Pardon, E., Valant, C., Sexton, P. M., Christopoulos, A., Felder, C. C., Gmeiner, P., Steyaert, J., Weis, W. I., Garcia, K. C., Wess, J., and Kobilka, B. K. (2013) Activation and allosteric modulation of a muscarinic acetylcholine receptor, *Nature 504*, 101-106.

[20] Abdul-Ridha, A., Lopez, L., Keov, P., Thal, D. M., Mistry, S. N., Sexton, P. M., Lane, J. R., Canals, M., and Christopoulos, A. (2014) Molecular determinants of allosteric modulation at the M1 muscarinic acetylcholine receptor, *J. Biol. Chem. 289*, 6067-6079.

[21] Ogino, K., Tokuda, Y., Nakai, T., and Tagaki, W. (1994) Hydrolysis of acetylcholine analogs catalyzed by an anionic surfactant containing 2-hydroxymethylimidazole and sulfate groups in the absence and presence of Cu2+ ion in mixed micellar systems, *Mem. Fac. Eng., Osaka City Univ. 35*, 187-197.

[22] Gould, R. G., and Jacobs, W. A. (1939) The Synthesis of Certain Substituted Quinolines and 5,6-Benzoquinolines, *J. Am. Chem. Soc. 61*, 2890-2895.

[23] de la Cruz, A., Elguero, J., Goya, P., Martínez, A., and Pfleiderer, W. (1992) Tautomerism and acidity in 4-quinolone-3-carboxylic acid derivatives, *Tetrahedron 48*, 6135-6150.

[24] Shindikar, A. V., and Viswanathan, C. L. (2005) Novel fluoroquinolones: design, synthesis, and in vivo activity in mice against Mycobacterium tuberculosis H37Rv, *Bioorg. Med. Chem. Lett. 15*, 1803-1806.

[25] Zhi, Y., Gao, L. X., Jin, Y., Tang, C. L., Li, J. Y., Li, J., and Long, Y. Q. (2014) 4-Quinolone-3-carboxylic acids as cell-permeable inhibitors of protein tyrosine phosphatase 1B, *Bioorg. Med. Chem. 22*, 3670-3683.

[26] Ziegler, N., Bätz, J., Zabel, U., Lohse, M. J., and Hoffmann, C. (2011) FRET-based sensors for the human M1-, M3-, and M5-acetylcholine receptors, *Bioorg. Med. Chem. 19*, 1048-1054.

[27] Maier-Peuschel, M., Frölich, N., Dees, C., Hommers, L. G., Hoffmann, C., Nikolaev, V. O., and Lohse, M. J. (2010) A fluorescence resonance energy transfer-based M2 muscarinic receptor sensor reveals rapid kinetics of allosteric modulation, *J. Biol. Chem. 285*, 8793-8800.

[28] Wess, J. (1998) Molecular basis of receptor/G-protein-coupling selectivity, *Pharmacol. Ther. 80*, 231-264.

[29] Tewson, P., Westenberg, M., Zhao, Y., Campbell, R. E., Quinn, A. M., and Hughes, T. E. (2012) Simultaneous detection of Ca2+ and diacylglycerol signaling in living cells, *PLoS One 7*, e42791.

[30] Bock, A., Merten, N., Schrage, R., Dallanoce, C., Batz, J., Kloeckner, J., Schmitz, J., Matera, C., Simon, K., Kebig, A., Peters, L., Müller, A., Schrobang-Ley, J., Tränkle, C., Hoffmann, C., De Amici, M., Holzgrabe, U., Kostenis, E., and Mohr, K. (2012) The allosteric vestibule of a seven transmembrane helical receptor controls G-protein coupling, *Nat. Commun. 3*, 1044.

[31] Bock, A., Chirinda, B., Krebs, F., Messerer, R., Batz, J., Muth, M., Dallanoce, C., Klingenthal, D., Tränkle, C., Hoffmann, C., De Amici, M., Holzgrabe, U., Kostenis, E., and Mohr, K. (2014) Dynamic ligand binding dictates partial agonism at a G protein-coupled receptor, *Nat. Chem. Biol. 10*, 18-20.

[32] Vilardaga, J. P., Steinmeyer, R., Harms, G. S., and Lohse, M. J. (2005) Molecular basis of inverse agonism in a G protein-coupled receptor, *Nat. Chem. Biol. 1*, 25-28.

[33] Hoffmann, C., Nuber, S., Zabel, U., Ziegler, N., Winkler, C., Hein, P., Berlot, C. H., Bunemann, M., and Lohse, M. J. (2012) Comparison of the activation kinetics of the M3 acetylcholine

receptor and a constitutively active mutant receptor in living cells, *Mol. Pharmacol. 82*, 236-245.

[34] Bock, A., Bermudez, M., Krebs, F., Matera, C., Chirinda, B., Sydow, D., Dallanoce, C., Holzgrabe, U., De Amici, M., Lohse, M. J., Wolber, G., and Mohr, K. (2016) Ligand Binding Ensembles Determine Graded Agonist Efficacies at a G Protein-coupled Receptor, *J. Biol. Chem. 291*, 16375-16389.

[35] Ilien, B., Glasser, N., Clamme, J. P., Didier, P., Piemont, E., Chinnappan, R., Daval, S. B., Galzi, J. L., and Mely, Y. (2009) Pirenzepine promotes the dimerization of muscarinic M1 receptors through a three-step binding process, *J. Biol. Chem. 284*, 19533-19543.

[36] Nayeem AA, K. A., Rahman MS, Rahman M. (2011) Evaluation of phytochemical and pharmacological properties of Mikania cordata (Asteraceae) leaves, *J. Pharmacognosy Phytother. 3*, 118-123.

[37] Leyva, E., Monreal, E., and Hernández, A. (1999) Synthesis of fluoro-4-hydroxyquinoline-3-carboxylic acids by the Gould–Jacobs reaction, *J. Fluor. Chem. 94*, 7-10.

[38] Niedermeier, S., Singethan, K., Rohrer, S. G., Matz, M., Kossner, M., Diederich, S., Maisner, A., Schmitz, J., Hiltensperger, G., Baumann, K., Holzgrabe, U., and Schneider-Schaulies, J. (2009) A small-molecule inhibitor of Nipah virus envelope protein-mediated membrane fusion, *J. Med. Chem. 52*, 4257-4265.

[39] Ho, S. N., Hunt, H. D., Horton, R. M., Pullen, J. K., and Pease, L. R. (1989) Site-Directed Mutagenesis by Overlap Extension Using the Polymerase Chain-Reaction, *Gene 77*, 51-59.

[40] Zürn, A., Zabel, U., Vilardaga, J. P., Schindelin, H., Lohse, M. J., and Hoffmann, C. (2009) Fluorescence resonance energy transfer analysis of alpha 2a-adrenergic receptor activation reveals distinct agonist-specific conformational changes, *Mol. Pharmacol. 75*, 534-541.

[41] Hoffmann, C., Gaietta, G., Zürn, A., Adams, S. R., Terrillon, S., Ellisman, M. H., Tsien, R. Y., and Lohse, M. J. (2010) Fluorescent labeling of tetracysteine-tagged proteins in intact cells, *Nat. Protoc. 5*, 1666-1677.

[42] Sletten, D. M., Nickander, K. K., and Low, P. A. (2005) Stability of acetylcholine chloride solution in autonomic testing, *J. Neurol. Sci. 234*, 1-3.

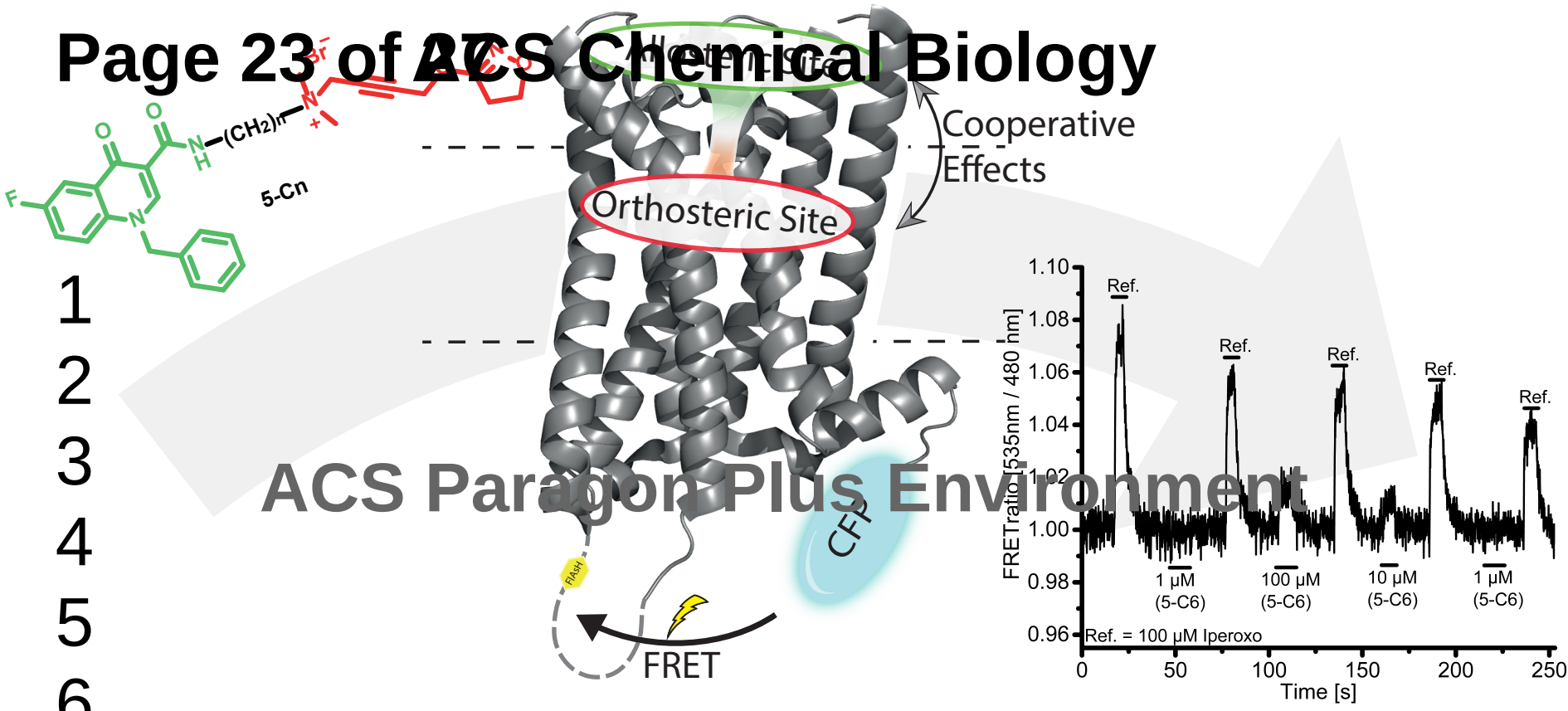

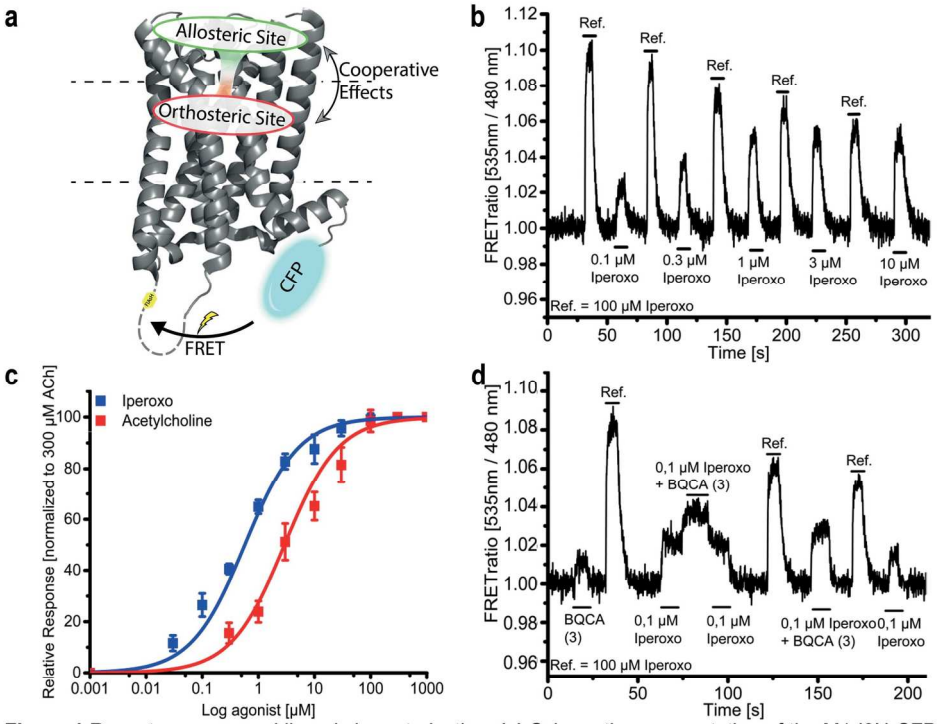

Figure 1 Receptor sensor and ligand characterization. **(a)** Schematic representation of the M1-I3N-CFP receptor sensor with insertion of the CCGPCC FlAsH-Binding site in intracellular loop 3 and fusion of CFP at the C-terminus. Schematically the allosteric and orthosteric regions for ligand binding are highlighted as well. **(b)** An example of a single cell FRET-recording of the M1-I3N-CFP stably expressed in HEK293 cells is shown. 100 µM iperoxo was used as reference ligand throughout the recording as indicated by black bars above the recorded signal. Different concentrations of iperoxo were applied as indicated at the appropriate time points by black bars underneath the recorded signal. The trace is representative of 30 cells measured at four different experimental days. Changes in FRET-ratio for 100 µM iperoxo varied between 9-11% at all cells **(c)** Concentration response curves of ACh (red, EC_{50} = 2.91 ± 0.07 µM) and iperoxo (blue, EC_{50} = 0.57 ± 0.02 µM) as calculated form FRET experiments using the M1-I3N-CFP receptor sensor. Each ligand concentration is represented by an average value of at least 10 cells. **(d)** 100µM iperoxo was used as reference throughout the recording as indicated by black bars above the recorded signal. Different concentrations and combinations of iperoxo and/or **3** were applied as indicated at the appropriate time points by black bars underneath the recorded signal. The trace is representative of 15 cells measured at four different experimental days.

Figure 1

165x196mm (300 x 300 DPI)

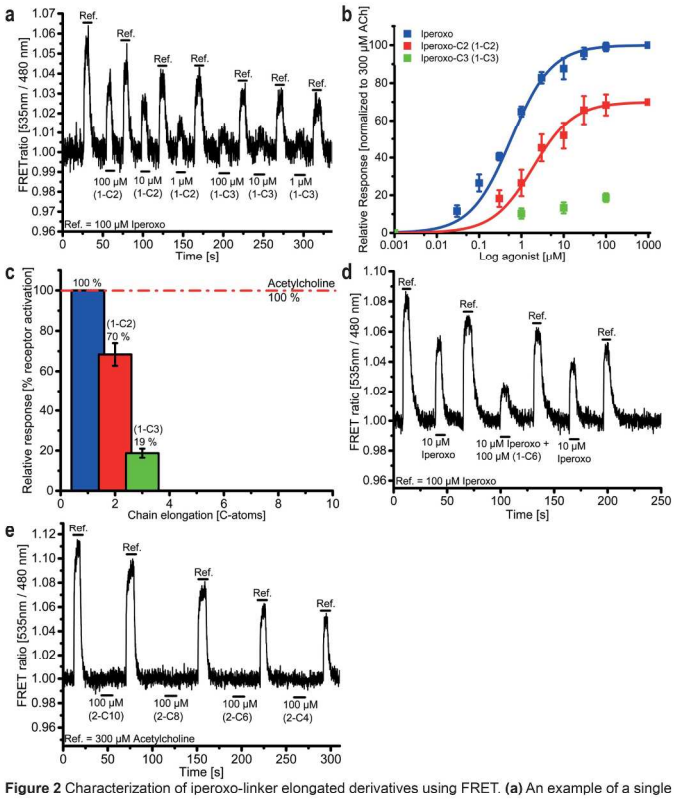

Figure 2 Characterization of iperoxo-linker elongated derivatives using FRET. **(a)** An example of a single cell FRET-recording of the M1-I3N-CFP stably expressed in HEK293 cells is shown. 100 µM iperoxo was used as reference throughout the recording as indicated by black bars above the recorded signal. Different concentrations of **1-C2** or **1-C3** were applied as indicated at the appropriate time pointsby black bars underneath the recorded signal. The trace is representative of 20 cells measured at three different experimental days. **(b)** Calculated concentration response curves of iperoxo (data from figure 1 c) and **1-C2** (EC50 = 1.67 ± 0.14 µM) are shown . Each ligand concentration is represented by an average value of at least 10 cells. For **1-C3** a 80% reduced conformational change was observed. **(c)** Observed FRET-response of linker elongated derivatives (**1-C2** to **1-C10**) as percent of control (100 µM iperoxo). Each bar represents the average of at least 10 independent measurements. **(d)** Ligand competition observed at a single cell level. 100 µM iperoxo was used as reference throughout the recording as indicated by black bars above the recorded signal. Application of 10 µM iperoxo alone or in combination with 100 µM **1-C6**, as indicated at the appropriate time points by black bars underneath the recorded signal, is indicative for binding of **1-C6** by reducing the effect of iperoxo in comparison to 10 µM iperoxo when applied alone. The trace is representative of 10 cells measured at three different experimental days. **(e)** 300 µM ACh was used as reference throughout the recording as indicated by black bars above the recorded signal. Maximal concentrations of **2-C4** to **2-C10** were applied as indicated at the appropriate time points and indicated by black bars underneath the recorded signal. The trace is representative of 15 cells measured at three different experimental days.

Figure 2

232x388mm (300 x 300 DPI)

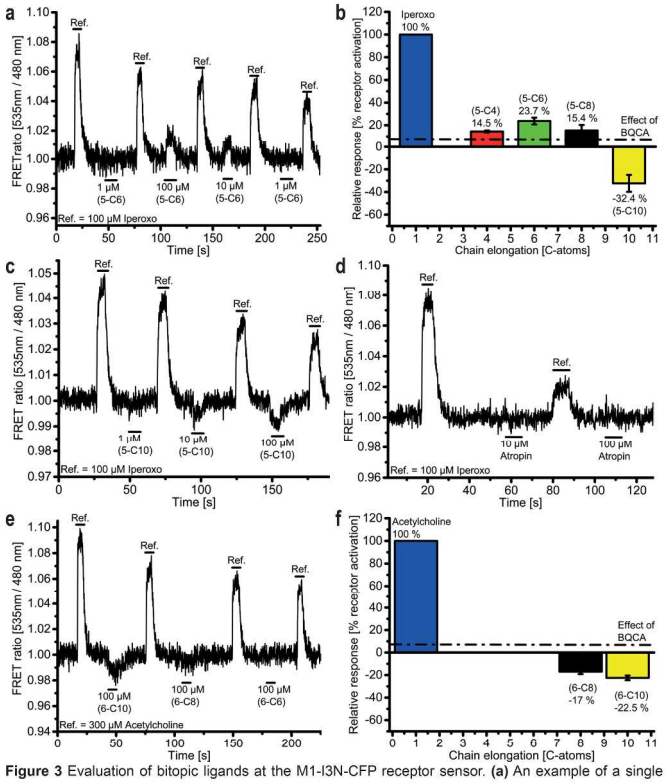

Figure 3 Evaluation of bitopic ligands at the M1-I3N-CFP receptor sensor. **(a)** An example of a single cell FRET-recording of the M1-I3N-CFP stably expressed in HEK293 cells is shown. 100 µM iperoxo was used as reference ligand throughout the recording as indicated by black bars above the recorded signal. Different concentrations of **5-C6** were applied as indicated at the appropriate time points by black bars underneath the recorded signal. The trace is representative of 20 cells measured at four different experimental days. The maximal detected signal for **5-C6** was 23.7 % compared to the reference. (b) Quantified maximal ligand induced FRET-response of compounds **5-C4** to **5-C10** as percent of control (100 µM iperoxo). Each bar represents the average of at least 10 independent measurements. **(c)** 100 µM iperoxo was used as reference ligand throughout the recording as indicated by black bars above the recorded signal. Different concentrations of **5-C10** were applied as indicated at the appropriate time points by black bars underneath the recorded signal. The trace is representative of 15 cells measured at three different experimental days. Note, the concentration dependent responses of **5-C10** showed an inverse signal direction compared to iperoxo. **(d)** The antagonist atropine did not induce a conformational change at the M1-I3N-CFP receptor sensor. **(e)** 300 µM ACh was used as reference ligand throughout the recording as indicated by black bars above the recorded signal. Different response to acetylcholine-based bitpopic ligands were determined for **6-C4** to **6-C10**. The trace is representative of 20 cells measured at four different experimental days. Acetylcholine based bitopic ligands results in an inverse FRET signal for derivatives with elongated chain length. **(f)** Quantified maximal ligand induced FRET-response of compounds **6-C4** to **6-C10** as percent of control (300 µM acetylcholine). Each bar represents the average of at least 10 independent measurements.

Figure 3

236x400mm (300 x 300 DPI)

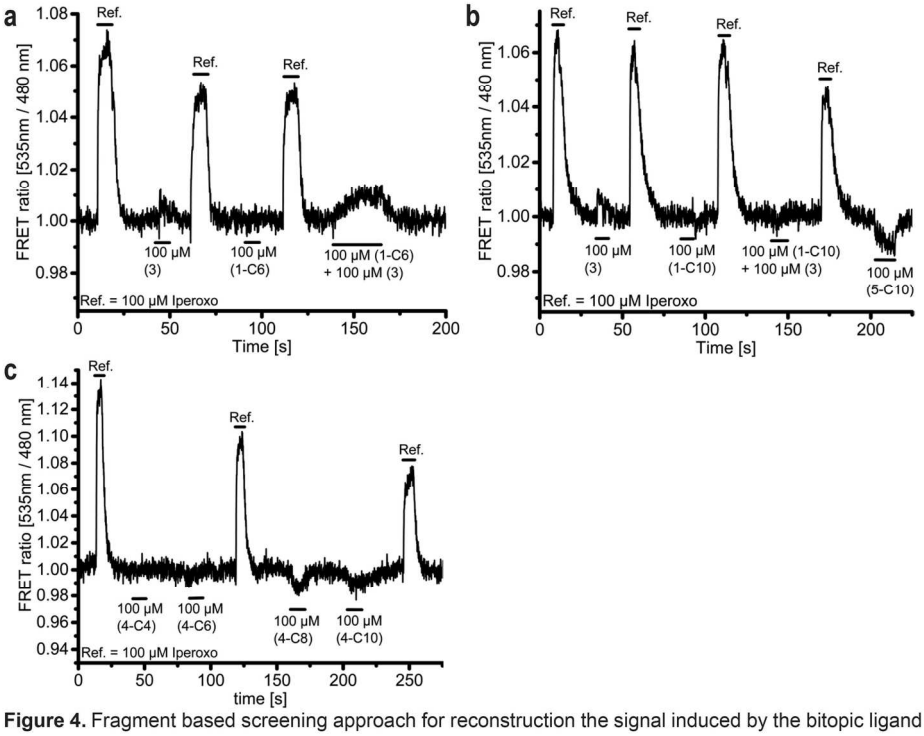

Figure 4. Fragment based screening approach for reconstruction the signal induced by the bitopic ligand by combining the individual components in one assay. **(a)** An example of a single cell FRET-recording of the M1-I3N-CFP stably expressed in HEK293 cells is shown. 100 µM iperoxo was used as reference ligand throughout the recording as indicated by black bars above the recorded signal. Alternatively, 100 µM of **(3)** and **(1-C6)** were applied separately or in combination as indicated at the appropriate time points by black bars underneath the recorded signal. Note, the combination of individual fragments **1-C6** and **3** leads to a similar signal amplitude as induced by **5-C6** (fig 3a). The trace is representative of 15 cells measured at three different experimental days. **(b)** 100 µM iperoxo was used as reference ligand throughout the recording as indicated by black bars above the recorded signal. Alternatively, 100 µM of **(3)** and **(1-C10)** were applied separately or in combination as indicated at the appropriate time points by black bars underneath the recorded signal. Note, the combination of individual fragments **1-C10** and **3** was not able to reproduce a similar signal amplitude as **5-C10**. The trace is representative of 15 cells measured at three different experimental days **(c)** 100 µM iperoxo was used as reference throughout the recording as indicated by black bars above the recorded signal. Maximal concentrations of **4-C4** to **4-C10** were applied as indicated at the appropriate time points and indicated by black bars underneath the recorded signal. The trace is representative of 15 cells measured at three different experimental days.

Figure 4

169x206mm (300 x 300 DPI)